



Trans. Nonferrous Met. Soc. China 27(2017) 584-590

Transactions of Nonferrous Metals Society of China

www.tnmsc.cn



Corrosion behavior of porous Ti₃SiC₂ in nitric acid and aqua regia

Xin-li LIU¹, Yao JIANG², Hui-bin ZHANG², Yue-hui HE²

- 1. School of Metallurgy and Environment, Central South University, Changsha 410083, China;
- 2. State Key Laboratory of Powder Metallurgy, Central South University, Changsha 410083, China

Received 29 June 2016; accepted 23 November 2016

Abstract: Porous Ti_3SiC_2 with high purity was synthesized using TiH_2 , Si and C powders with mole ratio of Ti to Si to C being 3:1.2:2 by reactive synthesis method. The corrosion behaviors of porous Ti_3SiC_2 in nitric acid and aqua regia were investigated by immersing test. Scanning electron microscope (SEM), X-ray diffractometer (XRD), energy dispersive spectrometer (EDS) and X-ray photoelectron spectroscopy (XPS) were used to analyze the morphology, compositions and element contents of the samples before and after corrosion to determine the corrosion product and corrosion mechanism. The mass loss values of porous Ti_3SiC_2 are 26.9 and 132.5 $\mu g/cm^2$, respectively after immersing in nitric acid and aqua regia for 600 h. The results indicate that Ti_3SiC_2 transforms to Ti_5Si_3 which has better corrosion resistance in nitric acid and aqua regia with mass loss values of 9.34 and 7.06 $\mu g/cm^2$ under the same immersing time, respectively. The dramatic dissolution of porous Ti_3SiC_2 in the acids is due to its special microstructure. **Key words:** porous Ti_3SiC_2 ; Ti_5Si_3 ; nitric acid; aqua regia; reactive synthesis; corrosion behavior; mass loss

1 Introduction

In recent years, a family of layered ternary metal ceramics called MAX phases (where M is transition metal; A is an A-group element, mostly IIIA and VIA; X is C or N element) have attracted much attention due to their unique physical and chemical properties [1,2]. In this family, the representative is Ti₃SiC₂. There has been a great interest in the synthesis and characterization of this material after being discovered by JEITSCHKO et al [3]. Ti₃SiC₂ has a hexagonal crystalline lattice with parameters a=0.3068 nm and c=1.7669 nm [3], and the crystalline structure shows a typical laminate characteristic [4]. The special crystal lattice and bond structures make the material combine prominent properties of both ceramics and metals [5]. Up to now, the methods mainly including chemical vapor deposition (CVD) [6,7],self-propagating high-temperature synthesis (SHS) [8,9], reactive sintering [10,11], hot isocratic pressing (HIP) [12,13], hot pressing (HP) [14,15], spark plasma sintering (SPS) [16,17] and mechanical alloying (MA) [18,19] have been used to synthesize Ti₃SiC₂. However, high-purity Ti₃SiC₂ is difficult to be synthesized, and the purity depends on the processing parameters [5]. Besides, various properties of the synthesized Ti₃SiC₂ have also been studied systematically. Corrosion resistance is a key factor that must be considered in the application of chemical industry and metallurgy. The corrosion behavior of Ti₃SiC₂ in various acids, alkali and salt has been extensively studied [20,21]. JOVIC et al [20] discovered that Ti₃SiC₂ was quite stable and passivated in HCl, H₂SO₄ and NaOH solutions. TRAVAGLINI et al [21] studied the corrosion behavior of Ti₃SiC₂ in various acids and NaOH, and concluded that Ti atoms dissolved and Si atoms were in-situ oxidized to form a SiO2-based layer on the surface, resulting in good corrosion resistance in acids. However, all the Ti₃SiC₂ reported is bulk material and the corrosion behavior in the strong oxidizing acids HNO₃ and aqua regia is not clear.

The corrosion behavior of porous materials in general, differed from that of the bulk materials of the same composition. Moreover, the pore morphology, porosity, pore size and pore surface condition also affect the corrosion process. A porous material was attacked not only on its surface but also from inside [22]. Although the excellent corrosion resistance of bulk Ti₃SiC₂ has

Foundation item: Projects (51604305, 51504296) supported by the National Natural Science Foundation of China; Project (2016M592445) supported by the China Postdoctoral Science Foundation; Project (169715) supported by the Postdoctoral Science Foundation of Central South University, China

been reported in Refs. [20,21], the corrosion behavior of porous Ti₃SiC₂ is necessary to be studied, and the variation of the pore structure should be considered, which is very important for the application of the porous material as a filter [23].

In this study, the corrosion behavior of porous Ti₃SiC₂ with high purity in HNO₃ solution and aqua regia was evaluated by immersing test. The microstructures and compositions before and after immersing in the solutions were characterized by SEM, EDS, XRD and XPS. The possible corrosion mechanism was proposed.

2 Experimental

2.1 Material synthesis

Porous Ti₃SiC₂ was prepared using commercially pure TiH₂, silicon and graphite powders as the starting materials. The purity of raw powders is 99.9% and their nominal composition is 72.1%TiH₂-16.3%Si-11.6%C with the mole ratio of Ti to Si to C being 3:1.2:2. Excessive silicon addition can make up for the evaporation loss of Si at high temperatures and ensure the purity of the samples. The powders were gently ball-mixed for 10 h using a powder rotator mixer, and then the mixed powders were formed into compact discs with dimensions of 30 mm × 3 mm under a pressure of 200 MPa at room temperature. The as-pressed compact discs were then sintered in a vacuum furnace with a pressure of 1×10⁻³ Pa using a step sintering method. During the heating process, the heating rate is 5 °C/min. The compacts were then initially sintered at 600 °C for 60 min to remove H from TiH₂. Then, the compact discs were held at 1350 °C for 3 h. The sintered discs were then cooled inside the vacuum furnace to the room temperature. Porous Ti₅Si₃ samples were also prepared by powder metallurgy method using TiH₂ and Si powders as the raw materials and finally sintered at 1200 °C for 2 h in the vacuum furnace.

2.2 Characterization

The macroscopic morphology of porous Ti_3SiC_2 was revealed by 3D X-ray microscope (Xradia VersaXRM–500–3D X-ray microscope). The specimens before and after immersing were characterized by field-emission scanning microscopy (Nova Nano SEM 230) equipped with an energy dispersive spectroscopy (EDS) system to study the morphology and compositions. The phase compositions of porous samples were analyzed by X-ray diffraction (XRD Dmax 2500VB) using a Cu K_{α} source. The open porosity of Ti_3SiC_2 was measured using Archimedes method and the pore size was determined on a porous material test instrument based on the bubble point method with N_2 as the fluid medium. The surface area of the porous Ti_3SiC_2

was measured using Brunauer–Emmett–Teller (BET) method (Monosorb, Quatachrome). The surface compositions of the samples were detected by X-ray photoelectron spectroscopy (XPS K-ALPHA)

2.3 Immersing test

The immersing tests were conducted at room temperature for 600 h. Five parallel samples were immersed in enough concentrated nitric acid (HNO₃, 68%, mass fraction), dilute nitric acid (HNO₃, 11%) and aqua regia to make sure the ratios for solutions and samples are larger than 20 mL/cm² according to standard ASTM NACE/ASTM G31–2012a [24]. The samples were periodically removed from solutions, rinsed in ultrasonic cleaner with deionized water and acetone 5 times respectively, and then dried in vacuum drying oven. Mass changes were measured on an analytical balance with a resolution of 0.1 mg for every cycle over a whole period.

3 Results and discussion

3.1 Characterization of synthesized porous Ti₃SiC₂

Figure 1(a) shows the macrograph of the synthesized porous specimen obtained layer by layer scanning with 3D X-ray microscope. From the edge of the image, it can be seen clearly that the pores are uniformly distributed in the whole body, and the overall and open porosities are 54.3% and 48.6% measured according to the Archimedes method, respectively. Figure 1(b) shows the SEM image of the porous sample, indicating that the pores are abundant. Figure 1(c) shows the pore diameter distribution of the porous sample, demonstrating that the average pore diameter is 6.2 µm, which is significantly narrower compared with most conventional porous metals, proving that the pore size of porous Ti₃SiC₂ is uniform. The specific surface area was measured to be 0.53 m²/g by BET method. Figure 1(d) shows the corresponding EDS spectrum, indicating that there are three elements Ti, Si and C, and the mass ratio of Ti to Si to C nearly the same as the element compositions of Ti₃SiC₂. Figure 2 shows the XRD patterns of the compacts before and after sintering. From the XRD patterns, we can find that after sintering, the raw materials of TiH2, Si and C (Fig. 2(a)) have completely transferred to Ti₃SiC₂ (JCPDS No. 74-0310). The purity of Ti₃SiC₂ calculated using the calibrated standard addition method [25] is 99.4%, much higher than the value reported previously [5].

3.2 Immersion test results

Mass loss curves from immersion testing in HNO₃ and aqua regia are plotted in Fig. 3. It is obvious that the mass of Ti₃SiC₂ is nearly constant in concentrated HNO₃

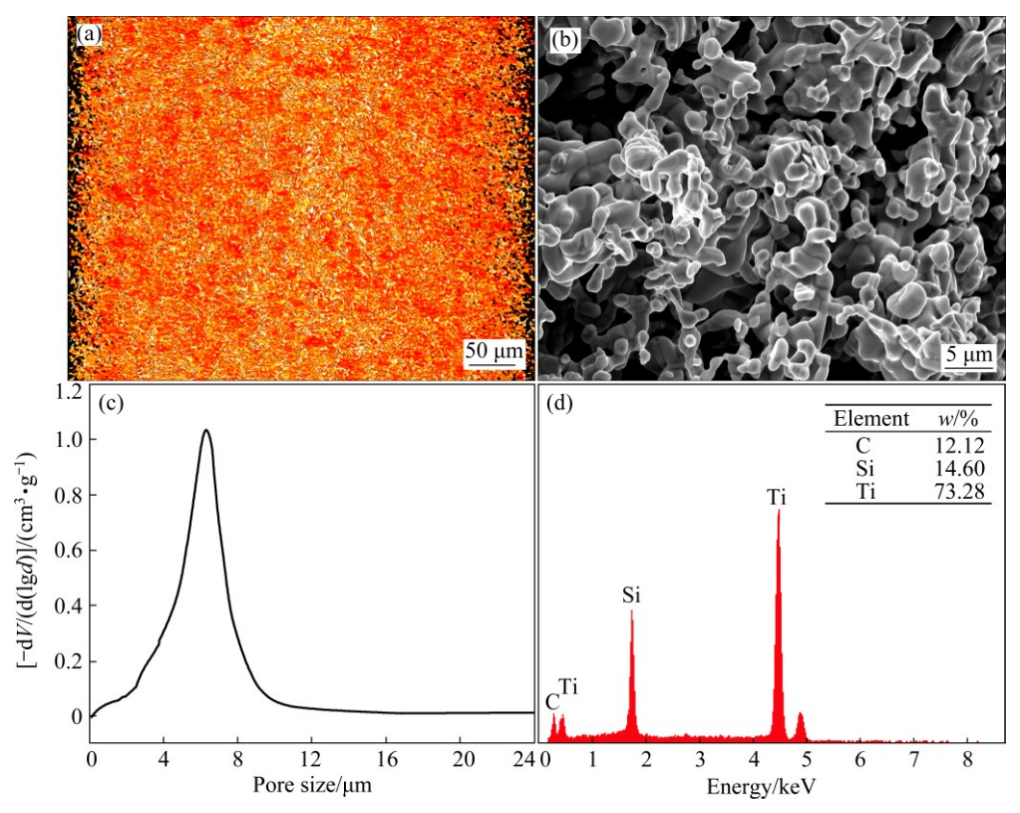


Fig. 1 Macrograph of synthesized porous Ti_3SiC_2 scanned layer by layer on 3D XRD microscope (a), SEM image (b), pore diameter distribution (c) and EDS spectrum (d)

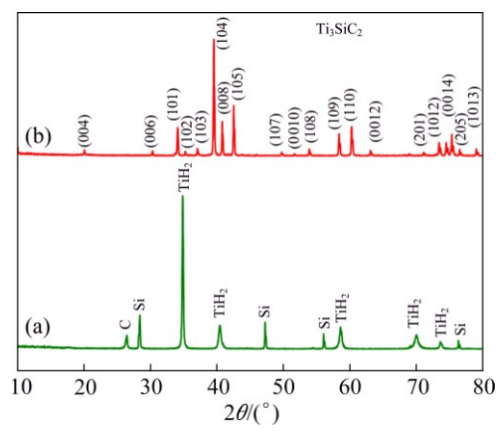


Fig. 2 XRD patterns of compacts before (a) and after (b) sintering

in the whole immersing period, while porous Ti_3SiC_2 dissolves much in dilute HNO_3 , as shown in Fig. 3(a). The mass loss increases uniformly along with the extending corrosion time. After immersing in dilute HNO_3 for 600 h, the mass loss reaches 26.9 $\mu g/cm^2$. In aqua regia, porous Ti_3SiC_2 exhibits a gradual dissolution and more dramatic mass loss (Fig. 3(b)), and the mass loss is 132.5 $\mu g/cm^2$ after immersing for 600 h.

3.3 Corrosion morphology

The morphologies of the samples after immersing in HNO₃ and aqua regia are shown in Fig. 4. It can be seen

that after immersing in dilute HNO₃, the specimen is not integrity as the original sample. Some skeletons of the porous Ti₃SiC₂ have been dissolved, presenting some obvious corrosion traces as shown in Fig. 4(a). The corresponding EDS pattern (Fig. 4(b)) including four elements, Ti, Si, C and O. O may be due to the oxidation layer produced on the surface of the specimen. Compared with the composition of original sample, mass ratios of Ti, Si and C change a lot. The mass ratios of Ti to C drop dramatically relative to the initial sample, while the mass ratios of Si to O have a significant increase. Figure 4(c) shows the SEM image of the sample after immersing in aqua regia. It is easy to find that some pores are blocked by the corrosion products and some oxide layers generate on the surface of the sample. The EDS results (Fig. 4(d)) also show that the contents of O and Si are high, while Ti and C contents have an obvious decline compared with that of the sample before immersing.

3.4 Corrosion composition

Figure 5 shows the XRD patterns of samples after immersing in dilute HNO_3 and aqua regia for 600 h. It can be seen from the XRD patterns that the samples after immersing in both solutions have some changes compared with the XRD pattern of original sample (Fig. 2(b)). Except for Ti_3SiC_2 phase, Ti_5Si_3 phase

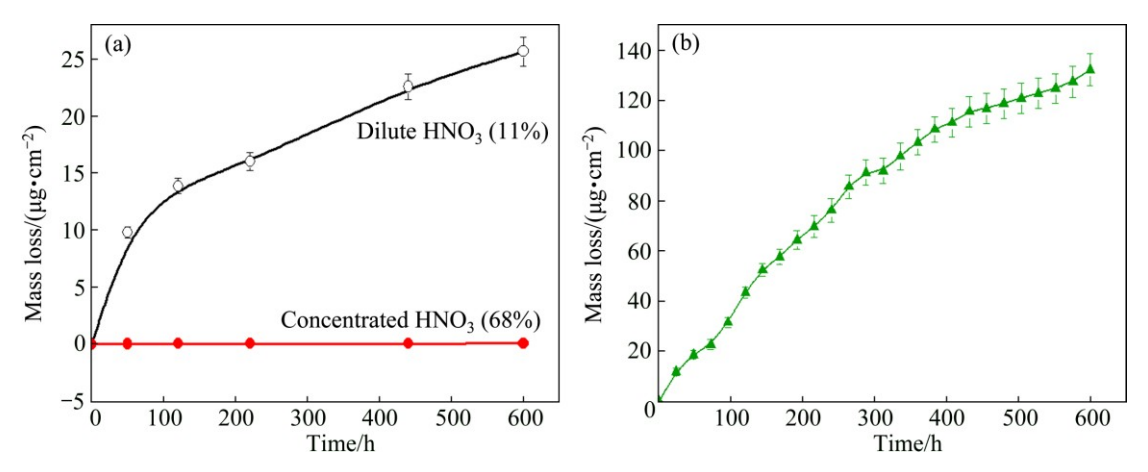


Fig. 3 Mass loss measurements of samples during immersing in HNO₃ (a) and aqua regia (b) for 600 h

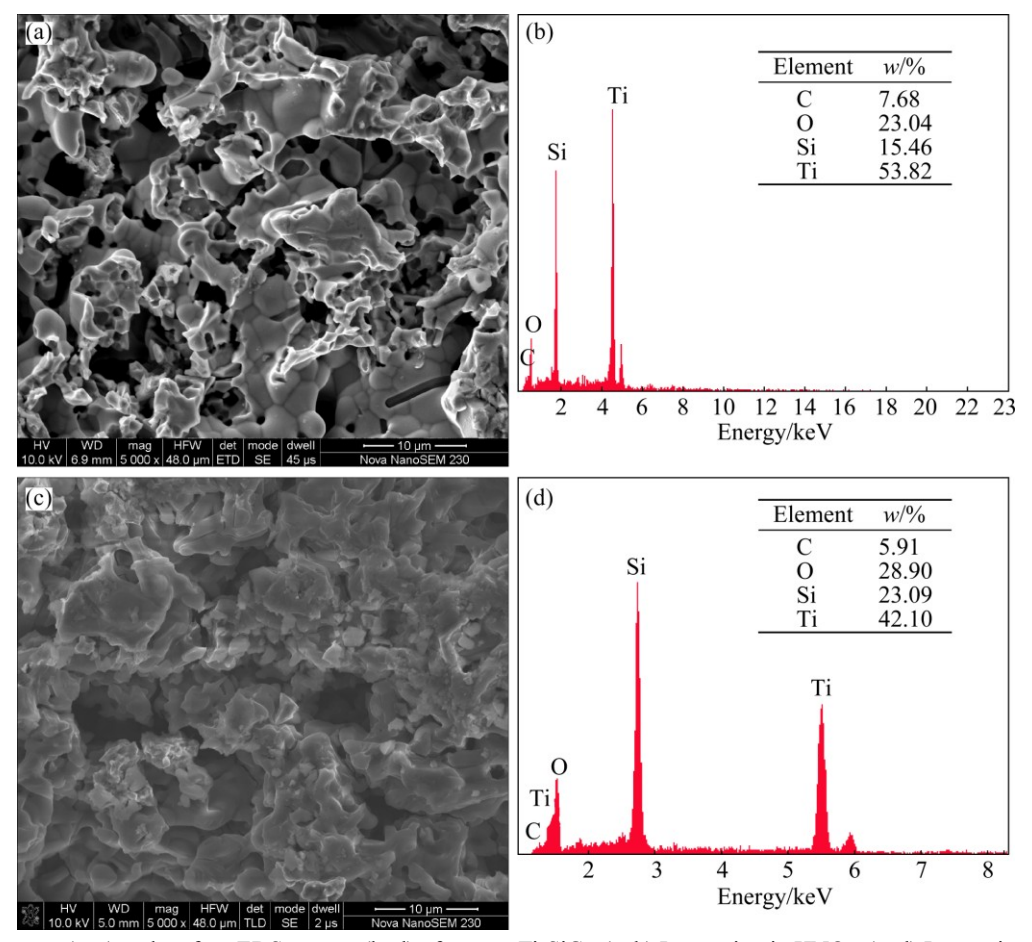


Fig. 4 SEM images (a, c) and surface EDS spectra (b, d) of porous Ti₃SiC₂: (a, b) Immersing in HNO₃; (c, d) Immersing in aqua regia

appears after immersing in dilute HNO_3 (Fig. 5(a)). It is noticeable that the composition of the sample almost completely changes from Ti_3SiC_2 to Ti_5Si_3 after immersing in aqua regia for 600 h, as shown in Fig. 5(b). Some amorphous phases are also present between 2θ values of $20^\circ-30^\circ$ in the XRD pattern. Combining the EDS analysis results, we can conclude that the amorphous products are SiO_2 or TiO_2 . In order to precisely determine the surface compositions, XPS

analysis (Fig. 6) was conducted to detect the surface compositions. The fitting curves of Si 2p at 103 eV for both specimens are attributed to the presence of SiO₂ [26]. The XPS spectrum of Ti 2p for the samples immersing in aqua regia exhibits two sets of peaks (464 and 459 eV), which are assigned to TiO₂. There is also a peak at 454 eV corresponding to Ti for the sample immersing in HNO₃, and this results from the Ti of raw material. The XPS spectra indicate that the surface

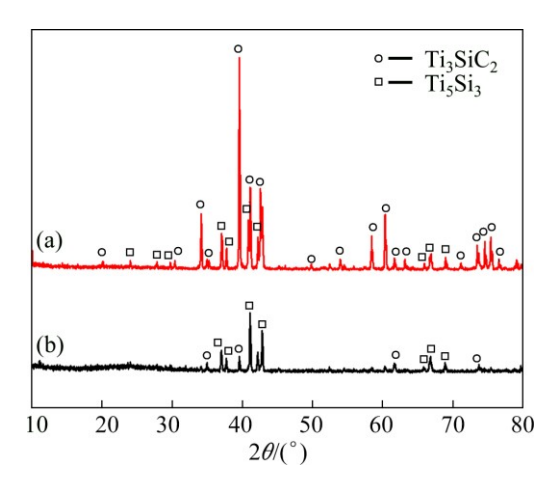


Fig. 5 XRD patterns of samples after immersing in dilute HNO₃(a) and aqua regia (b)

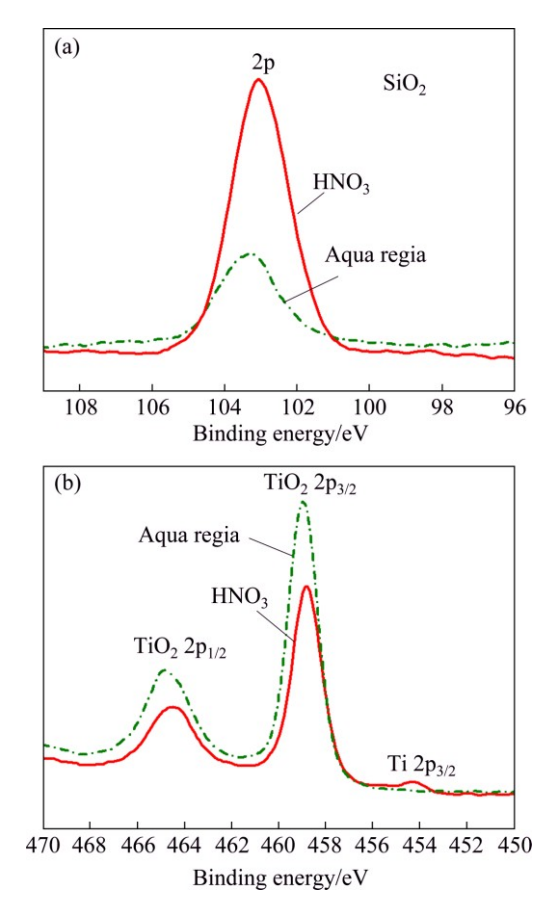


Fig. 6 XPS spectra of samples after immersing in HNO₃ and aqua regia for 600 h: (a) Si 2p; (b) Ti 2p

components of the samples contain SiO_2 and TiO_2 . It is evident that SiO_2 and TiO_2 generate after immersing in dilute HNO_3 and aqua regia and covered on the surface of samples. While most of the oxides have been dissolved in the immersing test, and cannot be detected by XRD.

3.5 Corrosion mechanism

The corrosion mechanism of metals in HNO3 has

been studied extensively [27–30]. EVANS [27] described a mechanism that explained the autocatalytic corrosion of metals in nitric acid medium. The high corrosion rate in HNO_3 is attributed to the main HNO_2 "electroactive" species that is involved in the autocatalytic reactions [28–30]:

$$2HNO_3 = 2HNO_2 + O_2 \tag{1}$$

$$HNO_2 + H^+ = NO^+ + H_2O$$
 (2)

$$NO^++e = NO$$
 (3)

$$NO+HNO_3=HNO_2+NO_2$$
 (4)

For low concentrations or at low temperature, the reduction of nitrous acid is the main electrochemical reaction and the final product is NO and this set of reactions generate depolarizing cations [28-30]. So, when the metals are immersed in HNO₃, the reduction of nitric acid will autoanalytically generate oxidants (oxidizing agent or oxidizer) like NO, NO2 and HNO₂ [29], and the dissolution of metals will be autocatalytic in nitric acid because cations are oxidized by solution which would be available for the nitric acid reduction, thus increasing the metal dissolution. Based on the above experimental results, we can conclude that the corrosion mechanism of the synthesized porous Ti₃SiC₂ in dilute HNO₃ and aqua regia is not exactly the same as the mechanism of metals in HNO3. From the SEM and XRD analysis, we can make an inference to explain for the dissolution procedure during the immersing test. Ti and C are firstly leached out and dissolved in 11% HNO₃ (mass fraction) and aqua regia like the dissolution of metal in lower concentration HNO3. Then, the residual Ti and Si recombine and generate Ti₅Si₃. As we know, there are two kinds of inequivalent Ti atoms in the Ti₃SiC₂ structure, which are usually referred as Ti1 and Ti2, where Ti1 occupies the (0, 0, z) position (Wyckoff position 2a) and Ti2 occupies the (1/3, 1/3, z) or (2/3, 2/3, z) positions (Wyckoff position 4f) [31]. It is found that Si (Ti2) and Ti2 (Si) show lower surface energies, indicating the most stable terminations at 0 K [31]. Ti-Si bond is the weakest in the Ti₃SiC₂ structure. So, in HNO₃ and aqua regia, Ti-Si bond is firstly destroyed and then single Ti-C bond is generated. The exposed Ti-C bond reacts with HNO3 and aqua regia and dissolves. ORELLANA and GUTIÉRREZ [31] also reported that the top surface Si (Ti2) exhibits a high mobility and the subsurface Ti atoms vibrate around their positions, keeping the structure geometry at high temperatures [31]. So, we can make a deduction that the exposed Si and Ti form Si—Si and Ti—Si bonds. The overall forming process is equal to reaction (5). The exposed Si would be oxidized in the strong oxidizing acid and produce SiO₂ passive coating which prevents further corrosion. The final corrosion product Ti₅Si₃ may be more stable than Ti₃SiC₂ in dilute

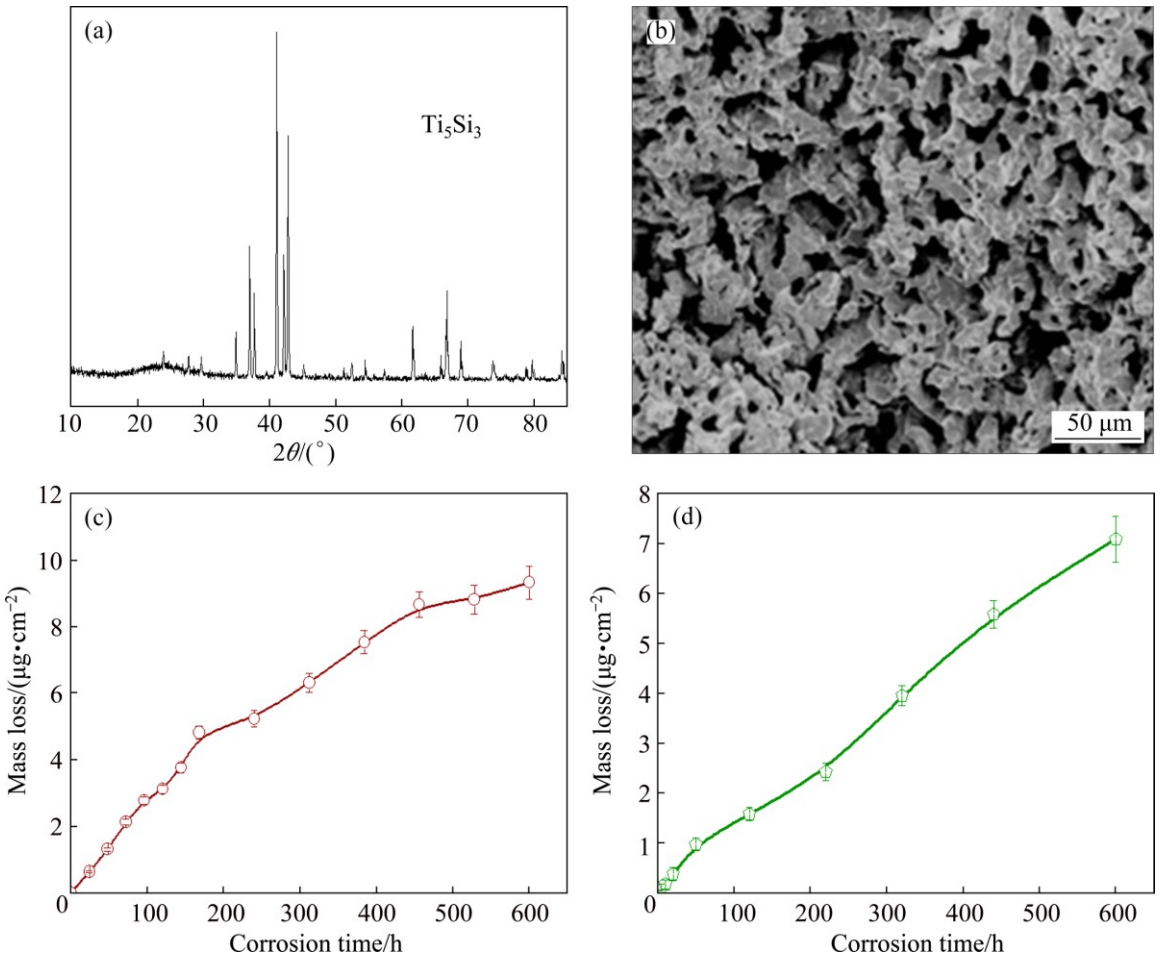


Fig. 7 XRD pattern (a), SEM image (b) of porous Ti₅Si₃, and mass lose of Ti₅Si₃ after immersing in 11% HNO₃ (c) and aqua regia (d) for 600 h

HNO3 and aqua regia.

$$5Ti_3SiC_2 = 10TiC + Ti_5Si_3 + 2Si$$
 (5)

In order to confirm the above deduction, porous pure Ti₅Si₃ with porosity of 50.3%, mean pore size of 8.5 µm was prepared. The XRD pattern and morphology of the synthesized porous Ti₅Si₃ are shown in Figs. 7(a) and (b), respectively. Porous Ti₅Si₃ samples were also immersed into dilute HNO3 and aqua regia for 600 h. Figures 7(c) and (d) show the mass loss plots of the samples immersed in 11% HNO₃ and aqua regia, respectively. The mass loss values of porous Ti₅Si₃ in 11% HNO₃ and aqua regia are 9.34 and 7.06 μg/cm² under the same immersing time of 600 h, respectively. It can be seen that the mass loss values of porous Ti₅Si₃ are much smaller than those of porous Ti₃SiC₂, especially in aqua regia. So, we can conclude that Ti₃SiC₂ decomposes into Ti₅Si₃ which has better corrosion resistance in dilute HNO₃ and aqua regia, while the decomposition product TiC dissolves into the solutions. This is coincident with the EDS patterns, in which C and Ti contents have a dramatical drop after immersing.

4 Conclusions

Porous Ti_3SiC_2 with purity of 99.4% was fabricated by reactive synthesis of TiH_2 –Si–C mixed powders. The corrosion behaviors of porous Ti_3SiC_2 in HNO₃ and aqua regia were investigated. After immersing in dilute HNO₃ and aqua regia for 600 h, the mass loss values are 26.9 and 132.5 $\mu g/cm^2$, respectively. Ti_3SiC_2 decomposes into Ti_5Si_3 which has better corrosion resistance in HNO₃ and aqua regia with mass loss values of 9.34 and 7.06 $\mu g/cm^2$ under the same immersing time of 600 h, respectively. The dramatic dissolution of porous Ti_3SiC_2 in HNO₃ and aqua regia is due to its special microstructure.

References

- WANG J Y, ZHOU Y C. Recent progress in theoretical prediction, preparation, and characterization of layered ternary transition-metal carbides [J]. Annual Review of Materials Research, 2009, 39: 415–443.
- AI Tao-tao. Research progress of layered conductive ceramic Ti₃SiC₂
 Journal of Ceramics, 2009, 30(2): 251–256.

- [3] JEITSCHKO W, NOWOTNY H, KRISTALLSTRUKTUR D. Ti₃SiC₂—A new complex carbide type [J]. Monthly Booklets for Chemistry and Related Parts of Other Sciences, 1967, 98: 329–337.
- [4] SUN Z M, MURUGAIAH A, ZHEN T, ZHOU A, BARSOUM M W. Microstructure and mechanical properties of porous Ti₃SiC₂ [J]. Acta Materialia, 2005, 53: 4359–4366.
- [5] ZHANG H B, BAO Y W, ZHOU Y C. Current status in layered ternary carbide Ti₃SiC₂: A review [J]. Journal of Materials Science and Technology, 2009, 25: 1–36.
- [6] GOTO T, HIRAI T. Chemically vapor deposited Ti₃SiC₂ [J]. Material Research Bulletin, 1987, 22: 1195–1201.
- [7] JACQUES S, DI-MURRO H, BERTHET M P, VINCENT H. Pulsed reactive chemical vapor deposition in the C-Ti-Si system from H₂/TiCl₄/SiCl₄ [J]. Thin Solid Films, 2005, 478: 13-20.
- [8] LI Jian-wei, XIAO Guo-qing. Mechanism research on selfpropagating high-temperature synthesis of Ti₃SiC₂ ceramics [J]. Powder Metallurgy Technology, 2007, 25(4): 271–280. (in Chinese)
- [9] RILEY D P, KISI E H, PHELAN D. SHS of Ti₃SiC₂: Ignition temperature depression by mechanical activation [J]. Journal of the European Ceramic Society, 2006, 26: 1051–1058.
- [10] RACAULT C, LANGLAIS F, NASLAIN R. Solid-state synthesis and characterization of the ternary phase Ti₃SiC₂ [J]. Journal of Materials Science, 1994, 29: 3384–3392.
- [11] YANG S, SUN Z M, HASHIMOTO H. Reaction in Ti₃SiC₂ powder synthesis from a Ti–Si–TiC powder mixture [J]. Journal of Alloys and Compounds, 2004, 368: 312–317.
- [12] BARSOUM M W, EL-RAGHY T. Synthesis and characterization of a remarkable ceramic: Ti₃SiC₂ [J]. Journal of the American Ceramic Society, 1996, 79: 1953–1956.
- [13] EL-RAGHY T, BARSOUM M W. Processing and mechanical properties of Ti₃SiC₂: I. Reaction path and microstructure evolution [J]. Journal of the American Ceramic Society, 1999, 82: 2849–2854.
- [14] LUO Y M, PAN W, LI S Q, LI J Q. Synthesis of high-purity Ti₃SiC₂ polycrystals by hot-pressing of the elemental powders [J]. Materials Letter, 2002, 52: 245–247.
- [15] RADHAKRISHNAN R, WILLIAMS J J, AKINC M. Synthesis and high-temperature stability of Ti₃SiC₂ [J]. Journal of Alloys and Compounds, 1999, 285: 85–88.
- [16] ZHANG Z F, SUN Z M, HASHIMOTO H. Rapid synthesis of ternary carbide Ti₃SiC₂ through pulse-discharge sintering technique from Ti/Si/TiC powders [J]. Metallurgical and Materials Transactions A, 2002, 33: 3321–3328.
- [17] ZHU Jiao-qun, MEI Bing-chu, CHEN Yan. Fabrication of Ti₃SiC₂ by spark plasma sintering from different raw materials [J]. Materials Science and Engineering, 2002, 20(4): 564–567. (in Chinese)

- [18] LI J F, MATSUKI T, WATANABE R. Combustion reaction during mechanical alloying synthesis of Ti₃SiC₂ ceramics from 3Ti/Si/2C powder mixture [J]. Journal of the American Ceramic Society, 2005, 88: 1318–1320
- [19] LI S, ZHAI H. Synthesis and reaction mechanism of Ti₃SiC₂ by mechanical alloying of elemental Ti, Si, and C powders [J]. Journal of the American Ceramic Society, 2005, 88: 2092–2098.
- [20] JOVIC V D, JOVIC B M, GUPTA S, EL-RAGHY T, BARSOUM M W. Corrosion behavior of select MAX phases in NaOH, HCl and H₂SO₄ [J]. Corrosion Science, 2006, 48: 4274–4282.
- [21] TRAVAGLINI J, BARSOUM M W, JOVIC V D, EL-RAGHY T. The corrosion behavior of Ti₃SiC₂ in common acids and dilute NaOH [J]. Corrosion Science, 2003, 45: 1313–1327.
- [22] ALVAREZ K, HYUN S K, TSUCHIYA H, FUJIMOTO S, NAKAJIMA H. Corrosion behaviour of lotus-type porous high nitrogen nickel-free stainless steels [J]. Corrosion Science, 2008, 50: 183-193.
- [23] LIU X L, ZHANG H B, JIANG Y, HE Y H. Characterization and application of porous Ti₃SiC₂ ceramic prepared through reactive synthesis [J]. Materials & Design, 2015, 79: 94–98.
- [24] ASTM NACE/ASTMG31-2012a. Standard guide for laboratory immersion corrosion testing of metals [S].
- [25] ZHANG Z F, SUN Z M, HASHIMOTO H. Rapid synthesis of ternary carbide Ti₃SiC₂ through pulse-discharge sintering technique from Ti/Si/TiC powders [J]. Metallurgical and Materials Transactions A, 2002, 33: 3321–3328.
- [26] WAGNER C D, RIGGS W M, DAVIS L E, MOULDER J F, MUILENBERG G E. Handbook of X-ray photoelectron srpectroscopy [M]. Minnesota: Perkin-Elmer Corporation, 1979.
- [27] EVANS U R. The corrosion and oxidation of metals [J]. Journal of Electrochemical Society C, 1961, 108: 94–95.
- [28] BALBAUDM F, SANCHEZ G, FAUVET P, SANTARINI G, PICARD G. Mechanism of corrosion of AISI 304L stainless steel in the presence of nitric acid condensates [J]. Corrosion Science, 2000, 42: 1685–1707.
- [29] KASPAROVA O V. Peculiarities of intergranular corrosion of silicon-containing austenitic stainless steels [J]. Protection of Metals, 2004. 40: 425–431.
- [30] NINGSHEN S, KAMACHI M U, AMARENDRA G, RAJ B. Corrosion assessment of nitric acid grade austenitic stainless [J]. Corrosion Science. 2009. 51: 322–329.
- [31] ORELLANA W, GUTIÉRREZ G. First-principles calculations of the thermal stability of Ti₃SiC₂ (0001) surfaces [J]. Surface Science, 2011, 605: 2087–2091.

多孔 Ti₃SiC₂ 在硝酸和王水中的腐蚀行为

刘新利1, 江垚2, 张惠斌2, 贺跃辉2

1. 中南大学 冶金与环境学院,长沙 410083; 2. 中南大学 粉末冶金国家重点实验室,长沙 410083

摘 要: 采用摩尔比为 3:1.2:2 的 TiH_2 、Si 和石墨粉末反应合成高纯度多孔 Ti_3SiC_2 。通过浸泡实验研究多孔 Ti_3SiC_2 在硝酸和王水中的腐蚀行为。采用扫描电镜、X 射线衍射、能谱仪和 X 射线光电子能谱仪分析样品腐蚀前后的形貌、成分和元素含量,确定腐蚀产物和腐蚀机制。结果表明: 多孔 Ti_3SiC_2 在稀硝酸和王水中腐蚀严重,浸泡 600 h 质量损失分别为 26.9 和 132.5 $\mu g/cm^2$, Ti_3SiC_2 在腐蚀过程中转化为 Ti_5Si_3 。而具有相似孔隙率和孔径的多孔 Ti_5Si_3 在硝酸和王水中浸泡 600 h 后质量损失分别为 9.34 和 7.06 $\mu g/cm^2$,表现出更好的抗腐蚀性。多孔 Ti_3SiC_2 在硝酸和王水中的腐蚀行为归因于其特殊的显微组织。

关键词: 多孔 Ti_3SiC_2 ; Ti_5Si_3 ; 硝酸; 王水; 反应合成; 腐蚀行为; 质量损失